Biochemical and Biophysical Research Communications **258,** 54–59 (1999)
Article ID bbrc.1999.0583, available online at http://www.idealibrary.com on IDEAL®

A New Assignment Strategy for the Hyperfine-Shifted ^{13}C and ^{15}N Resonances in Fe_2S_2 Ferredoxins

Nitin U. Jain and Thomas C. Pochapsky[1]
Department of Chemistry, Brandeis University, Waltham, Massachusetts 02254

Received March 11, 1999

Assignment of hyperfine-shifted resonances in paramagnetic metalloproteins such as Fe_2S_2 ferredoxins poses a major experimental challenge due to hyperfine shifts and/or severe line broadening. We have explored the possibility of using structural data from homologous proteins as part of an assignment strategy for the sequence-specific assignment of hyperfine-shifted backbone carbonyl ($^{13}C'$) and nitrogen resonances (^{15}N) in Fe_2S_2 ferredoxins. This strategy is based on the assignment of resonances in the paramagnetic region to particular types of amino acid residues using selective isotope labeling. Reduced metal–nuclear distances are then calculated from experimentally determined T_1 relaxation times for those resonances and the calculated distances aligned with the distances of nuclei at corresponding amino acid sequence positions in the crystal structure of a structurally homologous protein. The comparative assignment approach has met with success in correctly predicting the $^{13}C'$ and ^{15}N assignments in Pdx° from the crystal structure data of two similar and related ferredoxins, namely bovine adrenodoxin and *Anabaena* ferredoxin. Sequence-specific assignments made in this fashion were verified by selective $^{13}C'\{^{15}N\}$ decoupling experiments.

The ferredoxins form an important class of electron transfer proteins. The structure and function of these proteins have been under investigation for several decades. Putidaredoxin (Pdx) is a Fe_2S_2 ferredoxin from the camphor hydroxylation pathway of the soil bacterium *Pseudomonas putida* (1). The presence of unpaired electrons in the Fe_2S_2 cluster in both oxidation states at ambient temperatures makes the active site of Pdx and other Fe_2S_2 ferredoxins highly paramagnetic and difficult to investigate by NMR due to severe line broadening and hyperfine shifts. Sequence-specific assignments are usually impossible to make close to the metal centers of such ferredoxins using conventional ^1H-based multidimensional experiments. However, the relatively narrower line widths of ^{13}C, ^{15}N nuclei under the same conditions offer the possibility of obtaining sequence-specific assignments of the backbone and side-chain ^{13}C, ^{15}N resonances. By using an appropriate combination of samples selectively double- or multiple-labeled with $^{13}C'$ and ^{15}N at the backbone carbonyl and nitrogens, we were able to assign some of the $^{13}C'$ and ^{15}N resonances in Pdx sequence-specifically via difference decoupling experiments (2). This strategy has allowed us to investigate the redox dependence of hyperfine shifts and potential hydrogen bonding patterns of many of the residues in the Pdx metal binding site (2). Most of the remaining $^{13}C'$ and ^{15}N assignments for Pdx in the vicinity of the metal cluster have now been completed and are reported here.

Although the combination of selective labeling and decoupling experiments described here and in Ref. 2 forms an effective strategy for paramagnetic resonance assignment in ferredoxins, the process is in fact quite expensive and labor intensive. A much simpler and cost effective strategy would be quite useful. We now report the possibility of using structural data from structurally homologous proteins as part of such assignment strategy in Fe_2S_2 ferredoxins such as Pdx.

The solution structure of the oxidized form of Pdx (Pdx°) has been solved using NMR spectroscopy (3, 4). There is as yet no X-ray crystal structure available for Pdx. Due to severe line broadening and a lack of NOE constraints, the structure within a radius of 8 Å from the metal center was modeled from the crystal structure of a plant ferredoxin from *Anabaena* (5). Recently, a refined structure of Pdx° has been obtained using additional restraints for the diamagnetic region (6). The metal binding site and environs for this structure was modeled on the recently published crystal structure of a structurally similar ferredoxin, bovine adrenodoxin (Adx) (7). Adx has a greater homology to Pdx

[1] To whom correspondence should be addressed. E-mail: pochapsky@binah.cc.brandeis.edu. Website: http://pochapsky.chem.brandeis.edu.

Abbreviations used: NMR, nuclear magnetic resonance; Pdx, putidaredoxin; H-bonds, hydrogen bonds; $^{13}C'$, carbon of backbone carbonyl; [^{15}N], nitrogen of backbone amide; Pdx°, oxidized putidaredoxin; Adx, bovine adrenodoxin; T_1, longitudinal relaxation time.

0006-291X/99 $30.00

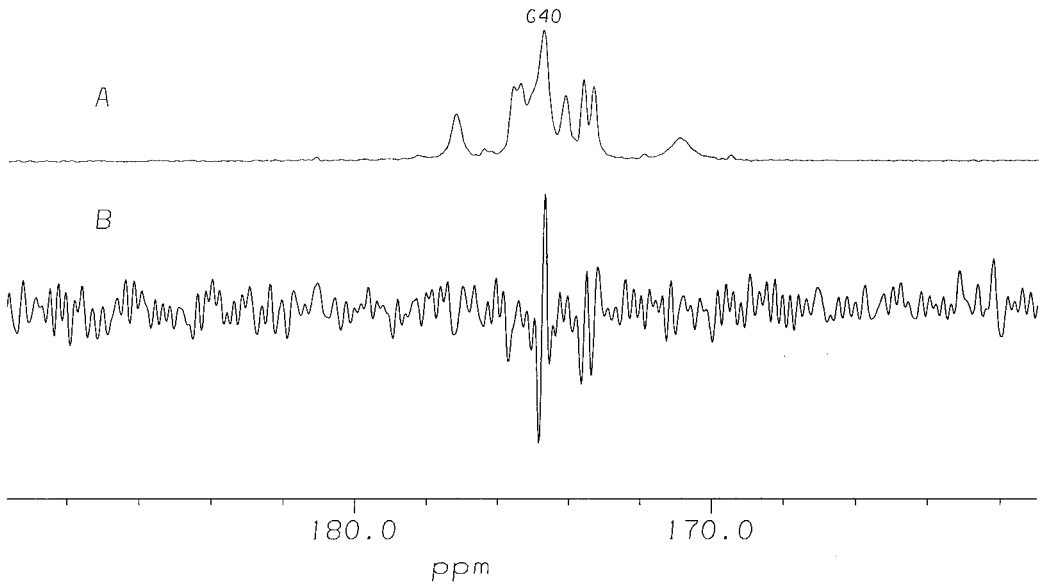

FIG. 1. (A) ^{13}C NMR spectrum of a Pdx° sample (pH 7.4, 10% D_2O, 290 K) selectively labeled with [$^{13}C'$] Gly (scrambled to [$^{13}C'$] Ser and [$^{13}C'$] Cys)/[^{15}N] Gly (scrambled to [^{15}N] Ser and [^{15}N] Cys); (B) Difference spectrum obtained by subtraction of a spectrum with selective decoupling at the ^{15}N frequency of neighboring Gly41 from a reference spectrum where the decoupler frequency was set off-resonance (~90 ppm). This assigns the $^{13}C'$ resonance of Gly40.

than does *Anabaena* ferredoxin in terms of both sequence and function. A high degree of structural similarity also exists between Pdx and Adx. However, there are differences in redox potentials and reactivities of ferredoxins even within the same class (8), and it is possible that small variations in the environment of the metal cluster can effect these changes. Whether such variations arise solely due to subtle structural changes (i.e., changes in the H-bonding pattern in the active site) or due to larger structural differences remains to be seen. For these reasons, it is useful to obtain an independent evaluation of the structural environment in the paramagnetic region.

One of the approaches frequently used for structural interpretation of hyperfine broadened and shifted NMR signals is to calculate a distance between a nucleus and metal center from paramagnetic contributions to nuclear relaxation. Alternatively, distances calculated from relaxation times have been used for making tentative assignments of paramagnetic resonances in several metalloproteins including ferredoxins and hemeproteins (9–11). However, recent attempts to correlate metal-nuclear distances with ^{15}N relaxation in Pdx° encountered difficulties due to a lack of unambiguous ^{15}N resonance assignments near the metal cluster (9, 12).

We have now made nearly complete unambiguous assignments for backbone $^{13}C'$ (carbonyl) and ^{15}N resonances of Pdx° using the double labeling strategy described previously (2). Three samples of selectively labeled Pdx° were prepared as follows: (1) [$^{13}C'$] Gly (scrambled to [$^{13}C'$] Ser and [$^{13}C'$] Cys) and [^{15}N] Gly (scrambled to [^{15}N] Ser and [^{15}N] Cys); (2) [$^{13}C'$] Gly (scrambled to [$^{13}C'$] Ser and [$^{13}C'$] Cys) and [^{15}N] Gln; (3) [$^{13}C'$] Gly (scrambled to [$^{13}C'$] Ser and [$^{13}C'$] Cys) and [^{15}N] Ala. Selective difference decoupling experiments were performed on these samples as described previously (Fig. 1) (2, 13). This allowed us to assign most $^{13}C'$ and ^{15}N backbone resonances in the paramagnetic region, with the exception of the $^{13}C'$ resonances of Thr47 and Gln87, and ^{15}N resonances of Cys39 and Cys48). Assignments are listed in Table 1.

Relaxation times for the assigned $^{13}C'$ (Fig. 2) and ^{15}N resonances were measured using an inversion recovery pulse sequence 180-τ-90 (Fig. 3). Longitudinal relaxation times T_1 were obtained from the initial slope of the plot of $\ln[I_0 - I_\tau/2I_0]$ vs $\ln[\tau]$ (13). ^{15}N T_1 values thus obtained are listed in Table 2 and those for $^{13}C'$ in Table 3. The relaxation time T_1 for a nucleus under paramagnetic influence is given by Eq. [1] (14):

$$\left(\frac{1}{T_1}\right) = \frac{2}{3}\left(\frac{A_c}{\hbar}\right)^2 S(S+1)\tau_s + \frac{4}{3}\left(\frac{\mu_0}{4\pi}\right)^2 \frac{\gamma_n^2 g_e^2 \mu_B^2 S(S+1)}{d^6}\tau_c + \left(\frac{\mu_0}{4\pi}\right)^2 \frac{4\omega_I^2 g_e^2 \mu_B^4 S^2 (S+1)^2}{(3kT)^2 d^6}\tau_c. \quad [1]$$

The first term in Eq. [1] corresponds to relaxation arising from the contact mechanism, the second from

TABLE 1

List of $^{13}C'$ and ^{15}N Assignments in the Paramagnetic Region of Pdx°

^{15}N resonances		$^{13}C'$ resonances	
δ (ppm)[a]	Assignment	δ (ppm)[b]	Assignment
109.5	G37[c]	174.8	G40[c]
117.6	G40[c]	175.0	G37[c]
156.2	G41[c]	175.4	G41[c]
132.1	S44	174.2	S42[c]
139.5	S42	175.2	S44[c]
131.0	A46[c]	173.5	A43
137.5	A43[c]	181.6	A46
151.0	C86[c]	171.0	C45[c]
136.2	C45[c]	173.4	C48[c]
135.4	C85	173.7	C86[c]
126.7	C39/C48[c]	175.7	C85[c]
107.2	C39/C48[c]	177.3	C39[c]

[a] All ^{15}N chemical shifts are reported relative to external liquid ammonia.

[b] All ^{13}C chemical shifts are reported relative to the methyl resonance of external DSS.

[c] New ^{15}N and $^{13}C'$ assignments reported in this work.

electron-nuclear dipolar interaction and the third from Curie spin relaxation, which is usually negligible for these systems (14). The contact term can be significant for nuclei directly bonded to the paramagnetic metal cluster. However, for nuclei such as $^{13}C'$ and ^{15}N that are at least three covalent bonds away from the metal cluster, the contact term is likely to be small and dipolar relaxation can be assumed to predominate. The dipolar relaxation term may then be used to estimate distances of nuclei from the metal cluster. For the current calculations, a value of 0.5×10^{-10} s for the correlation time τ_c was used, which is similar in magnitude to the value found in high spin Fe^{3+} ferredoxins (15). A weighted average spin number $<S_z>$ of 1.67 was used instead of $S(S + 1)$ to represent the population of various unpaired electronic spin states with increasing temperature (9). The distances then calculated by using the dipolar term in Eq. [1] are listed in Tables 2 and 3.

Reduced metal-nuclear distances were calculated for $^{13}C'$ and ^{15}N nuclei in the Adx structure using Eq. [2]:

$$d_r = \sqrt[6]{\frac{d_1^6 . d_2^6}{d_1^6 + d_2^6}} . \qquad [2]$$

In this equation, d_r is the reduced distance computed from d_1 and d_2, the distances between the nucleus and each of the two iron atoms. These reduced distances from Adx were then rank-ordered and compared with the rank-ordered distances calculated from experimentally determined $^{13}C'$ and ^{15}N T_1 values in Pdx°. These orderings were then used to make tentative assignments for the $^{13}C'$ and ^{15}N resonances of the nuclei in Pdx° (Tables 2 and 3). A comparison of tentative assignments with the actual assignments revealed that assignments made in this manner are largely incorrect. However, when resonances were grouped by

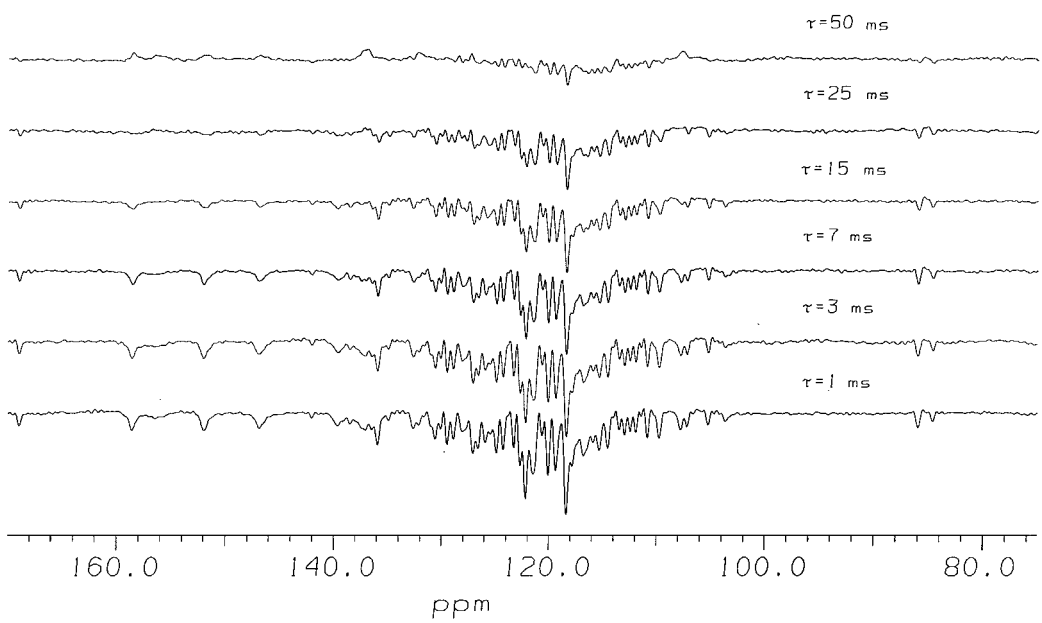

FIG. 2. T_1 relaxation measurements using the inversion recovery sequence [180-τ-90] (see text) on a [^{15}N] uniformly labeled sample. The corresponding value of τ used in the sequence is shown at the end of each spectrum. Spectra were also collected for other values of τ such as 5, 10, 20, and 30 ms (not shown in the figure).

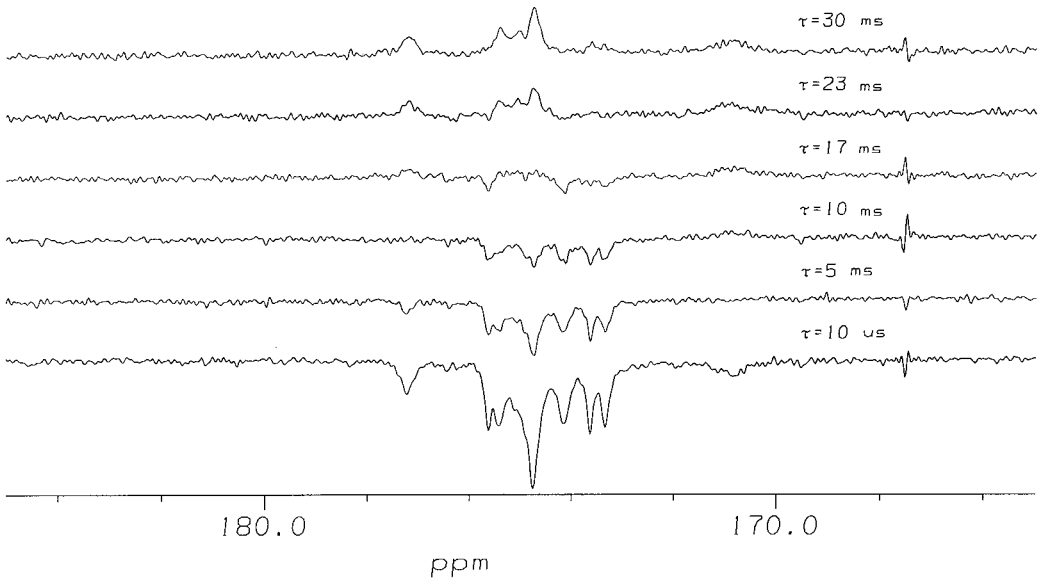

FIG. 3. T_1 relaxation measurements using the inversion recovery sequence [180-τ-90] (see text) on a [^{13}C′] Gly (scrambled to [^{13}C′] Ser and [^{13}C′] Cys) sample. The corresponding value of τ used in the sequence is shown at the end of each spectrum. Spectra were also collected for other values of τ such as 3, 7, 13, 20, 27, and 35 ms (not shown in the figure).

amino acid type (i.e., cysteines, glycines, serines, and alanines) and then aligned with the corresponding reduced distances in Adx, all of the relaxation-derived ^{15}N assignments matched the actual assignments. Similarly, except for Cys48 and Cys86, the ^{13}C′ tentative assignments matched the actual assignments. However, the distances determined for the ^{13}C′ nuclei of Cys48 and Cys6 from the T_1 values are within experimental error of each other, which may explain the observed discrepancy. The ^{15}N resonances of Cys39 and Cys48 have not been unambiguously assigned as yet by selective decoupling. However, based on the predicted assignments from the Adx structure, we tentatively assign the resonance at 107.2 ppm as that from the ^{15}N of Cys39 and the resonance at 126.7 ppm from the ^{15}N of Cys48. Efforts are currently under way to confirm these assignments via semiselective isotope labeling using intein-mediated peptide ligation (16).

These results imply that electron-nuclear dipole interactions are probably similar in analogous positions

TABLE 2

Comparison of the Actual ^{15}N Assignments in Pdx° with Predicted Assignments from Bovine Adrenodoxin and *Anabaena* Ferredoxin

δ (ppm)	T_1 value (ms)[c]	Putidaredoxin		Adrenodoxin		*Anabaena*	
		d Å[a]	Actual assignment	d_r Å[b]	Predicted assignment	d_r Å[b]	Predicted assignment
109.5	64	5.15	G37	5.28	G37	—	—
117.6	56	5.03	G40	4.49	G40	—	—
156.2	19	4.20	G41	4.04	G41	—	—
132.1	32	4.58	S44	4.10	S44	3.83	S44
139.5	47	4.89	S42	4.40	S42	4.05	S42
131.0	34	4.63	A46	4.50	A46	4.53	A46
137.5	30	4.54	A43	4.14	A43	3.76	A43
151.0	37	4.70	C86	4.17	C86	4.06	C86
136.2	22	4.31	C45	3.55	C45	3.51	C45
135.4	52	4.97	C85	5.20	C85	5.14	C85
126.7	58	5.06	C39/C48	4.28	C48	4.13	C48
107.2	29	4.51	C39/C48	3.88	C39	3.54	C39

[a] Distances in Pdx° calculated from T_1 values by using Eq. [1] with a precision of ±0.08 Å.
[b] Reduced distances calculated from crystal structure of Adrenodoxin and *Anabaena* ferredoxin using Eq. [2].
[c] Calculated from the mean of three measurements. Standard deviation of the mean is about ±2 ms.

TABLE 3

Comparison of the Actual ^{13}C Assignments in Pdx° with Predicted Assignments from Bovine Adrenodoxin and *Anabaena* Ferredoxin

δ (ppm)	T_1 value (ms)[c]	Putidaredoxin		Adrenodoxin		*Anabaena*	
		d Å[a]	Actual assignment	d_r Å[b]	Predicted assignment	d_r Å[b]	Predicted assignment
175.0	16	5.51	G37	4.82	G37	—	—
174.8	17	5.55	G40	5.03	G40	—	—
175.4	12	5.24	G41	4.53	G41	—	—
175.2	21	5.75	S44	4.47	S44	4.41	S44
174.2	32	6.17	S42	5.02	S42	4.68	S42
181.6	17	5.55	A46	5.06	A46	5.11	A46
173.5	15	5.44	A43	4.74	A43	4.57	A43
177.3	12	5.24	C39	4.30	C39	4.02	C39
171.0	6	4.67	C45	3.87	C45	3.90	C45
175.7	32	6.17	C85	5.34	C85	5.29	C48
173.4	22	5.80	C48	5.12	C86	4.90	C86
173.7	24	5.84	C86	5.16	C48	4.95	C85

[a] Distances in Pdx° calculated from T_1 values by using Eq. [1] with a precision of ±0.08 Å.
[b] Reduced distances calculated from crystal structure of adrenodoxin and *Anabaena* ferredoxin using Eq. [2].
[c] Calculated from the mean of three measurements. Standard deviation of the mean is about ±2 ms.

in structurally homologous proteins. This property can then be used to make tentative assignments for resonances in the paramagnetic region of homologous ferredoxins, first grouping resonances by residue type, then rank-ordering relaxation-derived distances and finally comparing those distances with those calculated from a homologous structure.

Our success in predicting resonance assignments for Pdx° from the Adx structure encouraged us to investigate the usefulness of this approach in predicting the set of Pdx° assignments from crystal structures from less homologous ferredoxins such as *Anabaena* ferredoxin (5). The sequence of Anabaena ferredoxin is shorter than that of Pdx by one amino acid residue in the interval between the first two ligand cysteines (analogous to Cys39 and Cys45 in Pdx) (Fig. 4). An accurate representation for Gly 40 and Gly 41 in Pdx therefore cannot be obtained from the *Anabaena* ferredoxin structure due to absence of an amino acid residue

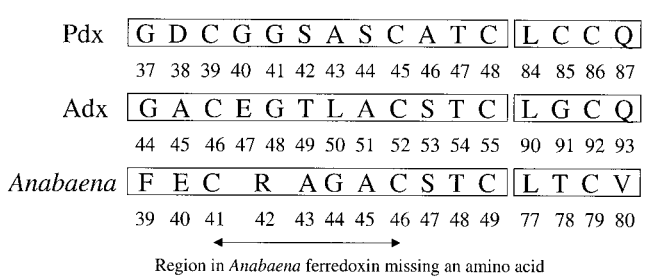

FIG. 4. Amino acid sequence in the paramagnetic region of putidaredoxin (Pdx), bovine adrenodoxin (Adx) and *Anabaena* ferredoxin.

at the corresponding position. We therefore decided not to include the glycines for the purpose of distance comparisons. Despite sequence differences, this approach still was able to predict the correct assignments for all the cysteine, serine and alanine $^{13}C'$ and ^{15}N resonances in the paramagnetic region of Pdx° (Tables 2 and 3). We were somewhat surprised to note that the correct assignments were predicted even for Ser42, Ala43, and Ser44, which are closest to the variant region in *Anabaena*. Apparently, the overall geometry of the ligating cysteines and the metal cluster remains basically the same in both proteins. This was also inferred from the observation that the metal center of the Pdx structure (in which the metal binding site was modeled from the *Anabaena* ferredoxin structure) essentially superimposes on the metal cluster of the Adx crystal structure (7). Taken together, these observations suggest that this assignment strategy will be general for the class of plant, bacterial and mammalian ferredoxins discussed here (17). However, this approach still needs to be tested with relaxation and structural data from other paramagnetic proteins as well. We are currently testing the validity of this approach in the assignments of Adx and terpredoxin (Tdx), another Fe_2S_2 ferredoxin that is structurally homologous to Pdx (18).

We expect that this assignment strategy, supplemented with a minimum number of difference decoupling experiments, should help in minimizing the expense and time required to make sequence-specific assignments in paramagnetic metalloproteins such as Fe_2S_2 ferredoxins.

ACKNOWLEDGMENTS

This work was supported by a grant from the National Institutes of Health (GM44191, T.C.P.). The authors thank Dr. Jurgen Muller (Max Delbrunck Institute, Berlin) for access to the crystallographic coordinates of bovine adrenodoxin.

REFERENCES

1. Gunsalus, I. C., and Wagner, G. C. (1978) *Methods Enzymol.* **52,** 166–188.
2. Jain, N. U., and Pochapsky, T. C. (1998) *J. Am. Chem. Soc.* **120,** 12984.
3. Ye, X. M., Pochapsky, T. C., and Pochapsky, S. S. (1992) *Biochemistry* **31,** 1961.
4. Pochapsky, T. C., Ye, X. M., Ratnaswamy, G., and Lyons, T. A. (1994) *Biochemistry* **33,** 6424.
5. Rypniewski, W. R., Breiter, D. R., Benning, M. W., Wesenberg, G., Oh, B. H., Markley, J. L., Rayment, I., and Holden, H. M. (1991) *Biochemistry* **30,** 4126.
6. Pochapsky, T. C., Jain, N. U., Kuti, M. K., and Lyons, T. A. (1999) *Biochemistry,* in press.
7. Muller, A., Muller, J. J., Muller, Y. A., Uhlmann, H., Bernhardt, R., and Heinemann, U. (1998) *Structure* **6,** 269.
8. Peterson, J. A., and Graham-Lorence, S. E. (1995) *in* Cytochrome $P450_{cam}$: Structure, Mechanism and Biochemistry, 2nd. ed., pp. 151–180, Plenum Press, New York.
9. Coxon, B., Sari, N., Holden, M. J., and Vilker, V. L. (1997) *Magn. Reson. Chem.* **35,** 743.
10. Chae, Y. K., and Markley, J. L. (1995) *Biochemistry* **34,** 188.
11. Bertini, I., and Luchinat, C. (1986) *in* NMR of Paramagnetic Molecules in Biological Systems (Lever, A. B. P., and Gray, H. B., Eds.), Benjamin/Cummings, Menlo Park.
12. Sari, N., Holden, M. J., Mayhew, M. P., Vilker, V. L., and Coxon, B. (1998) *Biochem. Biophys. Res. Commun.* **249,** 773.
13. All NMR ^{15}N and ^{13}C direct detection experiments were recorded at 290K on a Bruker AMX-500 spectrometer, operating at 50.68 and 125.76 MHz for ^{15}N and ^{13}C respectively, and equipped with a 5 mm broadband probe for heteronuclear detection. A typical ^{15}N or ^{13}C rapid acquisition experiment (recycling time $<$50 ms) consisted of 4K data points with a spectral width of 50,000 Hz. Broadband ^{1}H decoupling was used during all ^{15}N acquisitions. The rapid acquisition of signals allowed for the efficient detection of paramagnetic resonances due to suppression of the diamagnetic resonances. For the selective decoupling experiments, a modified Bruker triple resonance probe (doubly tuned to ^{15}N and ^{13}C in the inner coil) was used, allowing increased sensitivity for ^{13}C and ^{15}N. For the relaxation time measurements, a total recycling time of $\sim$ 300 ms was used. NMR data were processed and analyzed on Silicon Graphics workstations using Felix version 95.0 (Biosym, San Diego, CA) software.
14. La Mar, G. N., and de Ropp, J. S. *in* Biological Magnetic Resonance (Berliner, L. J., and Reuben, J., Eds.), Vol. 12, pp. 17–19.
15. Banci, L., Bertini, I., and Luchinat, C. (1990) *Struct. Bonding* **71.**
16. Jain, N. U., and Pochapsky, T. C. Unpublished results.
17. We have tested this approach on Pdx° with structural data from other similar Fe_2S_2 ferredoxins such as spinach ferredoxin and *spirulina platensis* ferredoxin (unpublished data) and the results are quite similar to that obtained with Adx and *Anabaena* ferredoxin.
18. Mo, H. M., Pochapsky, S. S., and Pochapsky, T. C. (1999) *Biochemistry,* in press.